

Fibrillar collagen scoring by second harmonic microscopy: A new tool in the assessment of liver fibrosis

Luc Gailhouste^{1,7}, Yann Le Grand^{2,6,7,†}, Christophe Odin^{2,7}, Dominique Guyader^{3,7}, Bruno Turlin^{4,7}, Frédéric Ezan^{1,7}, Yoann Désille^{3,7}, Thomas Guilbert^{2,7}, Anne Bessard^{1,7}, Christophe Frémin^{1,7}, Nathalie Theret^{5,7}, Georges Baffet^{1,7,*}

¹EA 4427 SeRAIC – INSERM U522, IFR 140, Université de Rennes 1, Hôpital Pontchaillou, 35033 Rennes, France; ²Institut de Physique de Rennes, UMR UR1-CNRS 6251, Université de Rennes 1, Campus de Beaulieu, 35042 Rennes, France; ³Liver Department Hôpital Pontchaillou, 35033 Rennes, France; ⁴Department of Pathology, Hôpital Pontchaillou, 35033 Rennes, France; ⁵EA SeRAIC – INSERM U620, IFR 140, Université de Rennes 1, 35043 Rennes, France; ⁶Laboratoire de Spectrométrie et Optique Laser, EA 938, Université de Bretagne Occidentale, 29238 Brest, France; ⁷Université Européenne de Bretagne, 5 Boulevard Laënnec, 35000 Rennes, France

See Editorial, pages 313–314

Background & Aims: Imaging of supramolecular structures by multiphoton microscopy offers significant advantages for studying specific fibrillar compounds in biological tissues. In this study, we aimed to demonstrate the relevance of Second Harmonic Generation (SHG) for assessing and quantifying, without staining, fibrillar collagen in liver fibrosis.

Methods: We first showed the relationship between SHG signal and collagen forms over-produced and accumulated during fibrosis progression. Taking this property into consideration, we developed an innovative method to precisely quantify the fibrosis area in histological slices by scoring of fibrillar collagen deposits (Fibrosis-SHG index).

Results: The scoring method was routinely applied to 119 biopsies from patients with chronic liver disease allowing a fast and accurate measurement of fibrosis correlated with the Fibrosis-Metavir score ($\rho = 0.75$, $p < 0.0001$). The technique allowed discriminating patients with advanced (moderate to severe) fibrosis (AUROC = 0.88, $p < 0.0001$) and cirrhosis (AUROC = 0.89, $p < 0.0001$). Taking advantage of its continuous gradation, the Fibrosis-SHG index also allowed the discrimination of several levels of fibrosis within the same F-Metavir stage. The SHG process presented several advantages such as a high reliability and sensitivity that lead to a standardized evaluation of hepatic fibrosis in liver biopsies without staining and pathological examination.

Conclusions: Second harmonic microscopy emerges as an original and powerful tool in the assessment of liver fibrosis and offers

new possibilities for the evaluation of experimental protocols. We expect that this technology could easily be applicable in the study of other fibro-proliferative pathologies.

© 2010 European Association for the Study of the Liver. Published by Elsevier B.V. All rights reserved.

Introduction

Chronic liver diseases are generally associated with extra-cellular matrix (ECM) over-production. Hepatic fibrosis is the result of a dynamic process characterized by an imbalance between fibrogenesis and fibrolysis responsible for the accumulation of fibrillar components in the liver such as fibrillar collagen [1]. The progression of human fibrosis may lead to cirrhosis and cancer with clinical complications followed by high morbidity and mortality rates particularly in chronic hepatitis B or C virus (HBV, HCV) infections [2,3]. In order to determine the degree of fibrosis, several methods are based on the pathological examination of liver biopsies by a trained pathologist using numerical systems with increasing severity stages like Scheuer [4], Ishak [5] or Metavir [6] scores after ECM staining [7,8]. The Metavir grading system appears well adapted for assessing chronic liver damage related to viral hepatitis. An alternative to the numerical scoring systems relies on a direct measurement of the amount of fibrotic deposits by morphometric image analysis [9,10]. To date, histomorphometric methodologies are not well standardized and appear to be time consuming procedures compared to classic numerical systems.

The aim of this study was to develop an innovative optical method for an accurate quantification of human liver fibrosis. This original process is based on an application of multiphoton microscopy enabling the observation of unstained samples using endogenous sources of nonlinear signals such as Two-Photon Excitation Fluorescence (TPEF) and Second Harmonic Generation (SHG). SHG makes the specific detection of supramolecules possible with high crystalline triple-helix structures deprived of centrosymmetry at microscopic and mesoscopic scales [11–14]. In biological tissues, fibrillar collagen displays these properties. Like

Keywords: Liver fibrosis; Fibrillar collagen; Fibrosis-SHG index; Multiphoton microscopy; Second Harmonic Generation.

Received 5 May 2009; received in revised form 8 September 2009; accepted 14 September 2009; available online 17 January 2010

* Corresponding author. Tel.: +33 22 323 4592.

E-mail address: georges.baffet@rennes.inserm.fr (G. Baffet).

† Present address: Laboratoire de Spectrométrie et Optique Laser, EA 938, Université de Bretagne Occidentale, 29238 Brest, France.

Abbreviations: ECM, extra-cellular matrix; HBV, hepatitis B virus; HCV, hepatitis C virus; TPEF, Two-Photon Excitation Fluorescence; SHG, Second Harmonic Generation; PSF, Point-Spread Function; PMT, photomultiplier tube; FITC, fluorescein isothiocyanate.



ELSEVIER

myosin fibers and microtubules, fibrillar collagen can generate a two-photon coherent process selectively collected and recorded at precisely half-wavelength of excitation which is characteristic of the SHG signature [15–18]. SHG microscopy has been successfully employed in various models and has revealed its high potential for imaging and analyzing fibrillar collagen in unstained tissues [19–22]. Recent data also suggested that SHG microscopy could be an interesting approach in the assessment of fibro-proliferative diseases [23,24].

In this study, we show that multiphoton microscopy using SHG provides a powerful tool for evaluating human liver fibrosis. We established a reliable and standardized method for the quantification of fibrillar collagen and analyzed the correlation between the Fibrosis-SHG index and the Fibrosis-Metavir score currently considered to be the gold standard in the clinical assessment of liver fibrosis.

Materials and methods

Biopsies and histological data

The study cohort included 119 patients who underwent percutaneous biopsies ($n = 73$) or large surgical biopsies ($n = 46$). Patients presented chronic liver disease with various degrees of severity related to HBV or HCV infection in 8.22% and 90.41% of cases, respectively; 1.37% presented co-infection with HBV and HCV. Exclusion criterion was inadequate specimen (length of biopsy <20 mm and/or portal tract <5). The mean biopsy length (percutaneous) was 39.6 ± 8.8 cm and mean number of fragments 2.4 ± 1.5 . Liver biopsies were performed by a senior operator using a 1.6-mm diameter needle. Biopsy specimens were fixed in formalin and embedded in paraffin. Liver histological status was assessed by the same trained pathologist, blind to the results of the SHG method, using the Fibrosis-Metavir scoring system. Fibrosis was staged on a scale from F0 to F4; F0 = no fibrosis, F1 = portal fibrosis without septa; F2 = few septa, F3 = numerous septa without cirrhosis, and F4 = cirrhosis.

Nonlinear microscopy imaging and SHG processing

To quantify SHG, we needed to precisely set up the experimental procedure. Multiphoton imaging was performed using 15 μm thick acute slices without de-waxing, staining, and cover slip. Acquisitions were taken with a 4 \times objective ($3.5 \times 3.5 \text{ mm}^2$) which enabled visualization of a major part of the slice. Furthermore, the axial extent of the Point-Spread Function (PSF) of the 4 \times objective, approximately 100 μm , made integrating SHG signals from the entire sample possible. Due to a reduced amount of material, needle biopsies were entirely imaged, whereas 10 non-overlapping acquisitions were randomly recorded on each large surgical biopsy. Excitation power and acquisition settings were chosen to achieve a trade-off between signal-to-noise ratio (SNR) and dynamics in SHG detection. Laser intensity was set at 100 mW and wavelength was fixed at 810 nm. Photomultiplier tubes (PMTs) were set at 800 V (PMT SHG) and 830 V (PMT TPEF). Circularly polarized laser pulses were sent to the microscope objective to ensure isotropic excitation of the sample regardless of the polarity of fibrillar collagen.

For long-term reproducibility of fibrillar collagen scoring, we calibrated our SHG set up on a selected region outside portal areas of a non-fibrotic slice (F0-Metavir) used as a reference before each measurement series. SHG scores were obtained from the surface density of pixels, presenting a level above an optimal threshold corresponding to 25% of the full intensity scale of the image. Optimal threshold value was determined on the basis of the intensity of the histograms of the SHG in the reference biopsy, which were found to exhibit a low intensity component. This signal is mainly attributed to the basal contribution of fibrillar collagen present in a normal liver.

Image processing and analysis (thresholding and SHG scoring) were routinely performed using macros established under ImageJ free software (v1.38x, National Institutes of Health, USA) and UCSD plugins, respectively, <http://rsb.info.nih.gov/ij> and <http://rsb.info.nih.gov/ij/plugins>. A 3-D reconstruction was generated with the VolumeJ plugin of ImageJ. We provide technical information on multiphoton microscope set up as well as a detailed protocol for fibrillar collagen quantification (SHG scoring macro under ImageJ software) in [Supplementary methods](#). The complete program for SHG scoring under ImageJ ("ready to run") is available on request from the corresponding author.

Immunohistochemistry assays were performed with formalin fixed sections of large surgical biopsies from normal and cirrhotic livers (respectively, F0 and F4-Metavir, 5 μm thick). Samples were incubated with ODYSSEY blocking buffer for 1 h (Li-COR Biosciences, USA). Then, sections were exposed, respectively, to collagen I, collagen III (PS060 and PS062, MONOSAN, The Netherlands) or collagen IV (sc-59814, Santa Cruz Biotechnology, USA) antibodies over night. Immunolabelings were revealed using the appropriate secondary antibody coupled with fluorescein isothiocyanate (FITC, sc-2078 and sc-2012, Santa Cruz Biotechnology, USA). Simultaneous TPEF and SHG images were collected with an excitation wavelength at 810 nm to compare SHG signals with immunolabeling (TPEF channel). Colocalization between SHG and TPEF was established using the colocalization module of ImageJ.

Statistics

The Mann-Whitney test was used for the estimation of Fibrosis-SHG indexes statistical difference between Metavir stages. The p -values were two-tailed. Statistical assessment for Mann-Whitney tests, Spearman's coefficient of rank correlation and operating curve analysis were performed using MedCalc software (Mariakerke, Belgium). A result was considered to reach statistical significance at $p < 0.05$.

Results

Multiphoton microscopy in human liver fibrosis

The SHG phenomenon within molecules exhibiting non-centrosymmetric organization is characterized by a change of the excitation energy from two infrared incident photons into one emerging visible photon at exactly twice the energy (precisely half of the excitation wavelength) (Fig. 1A). In order to illustrate the high potential of multiphoton microscopy, we first imaged liver with moderate fibrosis (F2-Metavir). Liver cryosections (100 μm thick) were made and imaged without staining, at mid-depth, to collect simultaneously endogenous TPEF and SHG signals. During acquisitions, excitation wavelength was set at 810 nm and specific barrier filters were used to separately collect the specific endogenous signals at 405 nm for the SHG (transmission mode) or the entire autofluorescence (epicollection mode). TPEF imaging at low magnification (10 \times) showed the typical autofluorescence of liver (Fig. 1B), while the 60 \times objective provided resolution at the micrometer scale inside the sample (mid-depth) and without the use of any staining (Fig. 1E). The SHG response selectively visualized with the 405 nm bandpass filter revealed fibrillar components of ECM. Low enlargement (10 \times) mainly displayed the strong localization of SHG within the stroma of portal tracts (white arrows in Fig. 1C), whereas 60 \times focus highlighted ECM distribution inside liver parenchyma (Fig. 1F). More importantly, simultaneous TPEF and SHG imaging clearly revealed ECM distribution around hepatocytes and demonstrated the complementarity between these two imaging modalities (Fig. 1G). In addition, multiphoton microscopy by SHG enabled high in-depth imaging with strong z -sectioning and spatial resolution allowing 3-D reconstruction of the ECM network as presented in Fig. 2. The 3-D reconstructions exhibited ECM network connections and arrangement in all liver parenchyma at a micrometer scale (Fig. 2C and Video S1). Such reconstructions were routinely done on thick liver slices, at depths up to 200 μm , permitting a precise study of ECM organization at the cellular level without particular tissue preparation.

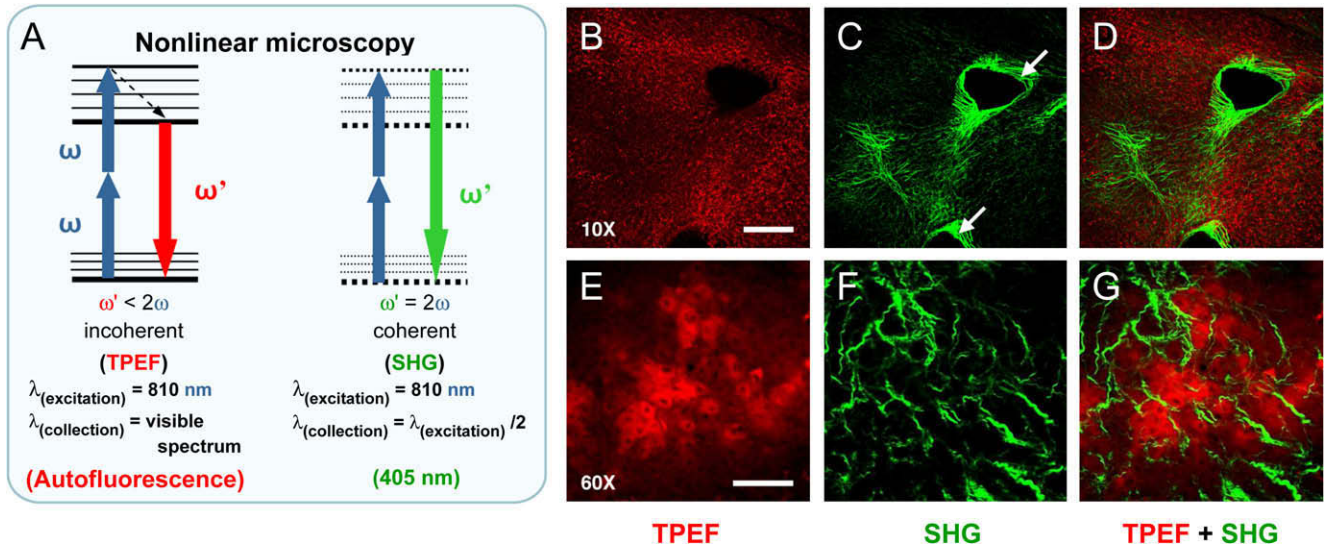


Fig. 1. Nonlinear microscopy in human fibrotic liver. (A) SHG and TPEF imaging principle (energy diagrams) with specific wavelengths of excitation and collection used for acquisitions. (B and E) Typical TPEF recorded with 10× and 60× at mid-depth (50 μm) displayed in red pseudocolor. (C and F) SHG signals collected using a band pass filter at the second harmonic wavelength (405 nm) with 10× and 60×. SHG is shown in green pseudocolor. (D and G) Simultaneous TPEF and SHG imaging. Circular polarization has been used for all acquisitions and laser intensity set at 50 mW (10×) and 25 mW (60×). Scale bars are, respectively, 250 and 60 μm with 10× and 60× magnification.

SHG microscopy allows specific imaging of fibrotic deposits in the liver

Immunohistochemistry assays were performed to analyze the specificity of SHG signals for fibrillar compounds involved in liver

fibrosis (mainly formed by fibrillar collagen I and III). First, TPEF and SHG were recorded by focusing on the same portal area, displaying a large amount of collagen, in serial sections of a normal liver (F0-Metavir). As demonstrated in Fig. 3A, collagen I immunolabeling is essentially located in the adventitia (TPEF) and co-localized perfectly with the SHG signal. Collagen III also co-localized with SHG and displayed a similar distribution to collagen I. On the contrary, collagen IV (non-fibrillar) showed a restricted distribution into the basal lamina but never co-localized with SHG. Furthermore, we performed the same experiments in highly fibrotic liver in order to confirm the specificity of SHG for fibrillar collagen in the case of liver fibrosis development. In cirrhotic liver (F4-Metavir), SHG signal also strongly co-localized with fibrillar collagen type I (Fig. 3B) and type III, whereas no significant correlation was found for collagen IV (see Fig. S1 as supporting data for collagen III and IV immunoassays in F4 samples). As a result, SHG imaging allows the specific examination of the main types of fibrillar supramolecules involved in liver fibrosis.

SHG imaging in the assessment of human liver fibrosis

In order to characterize the evolution of fibrillar collagen deposits in the development of human hepatic fibrosis, SHG imaging has been performed on liver biopsies taken from patients who had different grades of fibrosis ranging from portal fibrosis (F1-Metavir) to cirrhosis (F4-Metavir). First, SHG imaging clearly revealed the increase of fibrillar collagen amount during fibrosis progression and offered the possibility of an accurate characterization of its evolution without specific staining as shown in Fig. 4A. Thus, early fibrosis grades were characterized by an accumulation of fibrillar collagen in portal tracts. Later stages exhibited an increase of septa deposits and a dramatic augmentation of fibrillar collagen areas. We then compared second harmonic microscopy to linear imaging performed after Sirius red staining used for the Metavir (F3-Metavir biopsy in Fig. 4B). SHG images

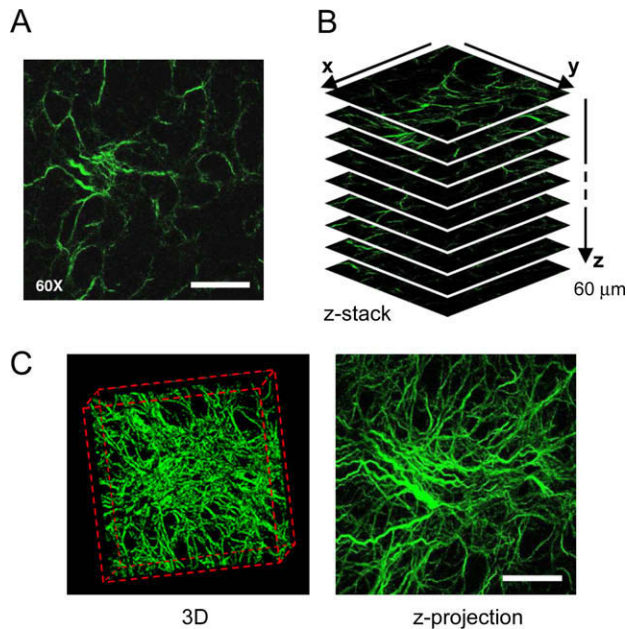


Fig. 2. 3-D imaging by SHG in human fibrotic liver. (A) SHG image recorded at mid-depth of a fibrotic biopsy section. (B) SHG z-stack generated with 1 μm step size (0–60 μm deep). (C) ECM network reconstruction in the three dimensions (xyz) and z-projection of SHG signals collected in the entire volume imaged (235 × 235 × 60 μm³). Circular polarization has been used for acquisitions with 25 mW laser input, 810 nm wavelength excitation and 60× objective. Scale bar is 60 μm. See Video S1 for z-stack acquisition.

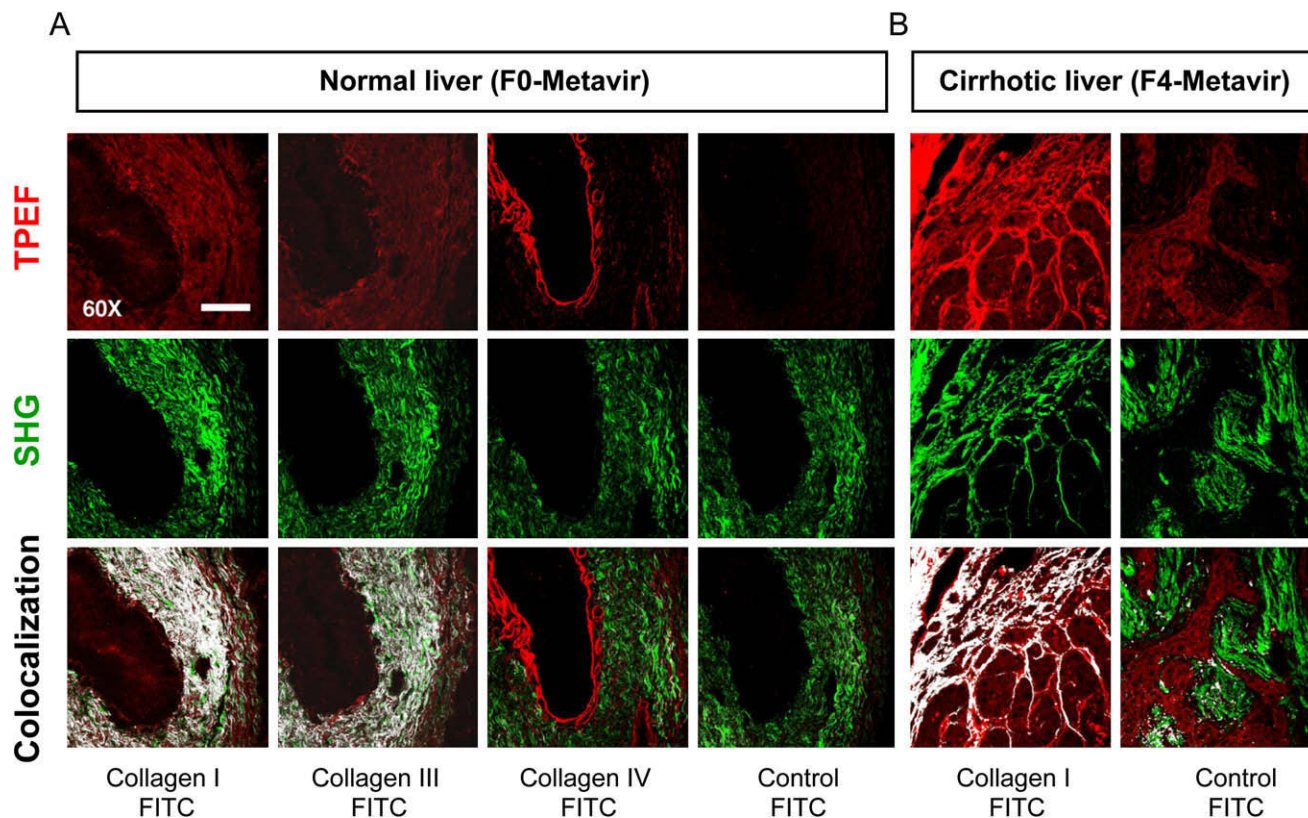


Fig. 3. SHG specificity for fibrillar collagen in liver. The specificity of SHG signals for fibrotic deposits (fibrillar collagen type I and III) in liver has been analyzed by immunohistochemistry assays. (A) Portal area immunolabeling imaged by TPEF and SHG in serial sections of a normal liver (F0-Metavir). (B) Immunoassays performed in highly fibrotic parenchyma of a cirrhotic liver (F4-Metavir). Unlabelled sections have been used as control and colocalization (merging) between SHG and immunostaining (TPEF channel) generated in white pseudocolor. Laser excitation: 25 mW with 810 nm wavelength; 60× objective; Scale bar: 50 μm. See Fig. S1 for fibrillar collagen type III and non-fibrillar collagen type IV immunoassays in cirrhotic samples.

displayed a strong signal within portal tracts and septa; likewise, so did the acquisitions after staining. However, in fibrotic parenchyma (dotted squares) Sirius red did not present a significant signal due to the strong background whereas SHG imaging showed an important distribution of fibrillar collagen. SHG provided higher signal-to-background contrast and resolution because of the absence of signal from the hepatocyte. Moreover, we recorded the emission spectra in high and low fibrotic areas to analyze the relationship between SHG intensity under 810 nm excitation and the amount of fibrillar collagen (Fig. 4C). The spectral response of the low fibrotic region was characterized by a small peak at the second harmonic wavelength (405 nm). On the other hand, the spectrum exhibited a 7-fold higher SHG intensity in highly fibrotic areas. Remarkably, no significant modification was observed in the TPEF response between high and low fibrotic regions.

Liver fibrosis assessment using the Fibrosis-SHG index

In this study, we aimed to demonstrate the capacity of second harmonic microscopy for evaluating human liver fibrosis by a precise quantification of fibrillar collagen using SHG scoring. As described in Materials and Methods, we developed a protocol in order to obtain a binary distribution of the SHG signal from surgical (Fig. 5A) and needle biopsies (Fig. 5B). Importantly, normal structural collagen in parenchyma and portal tracts was excluded

from analysis after the thresholding process (binary SHG) which allowed the specific quantification of pixels with significant fibrosis. The scoring method was routinely applied to the 119 liver biopsies of this study and SHG scores analyzed considering the F-Metavir stages assigned by the pathologist (see Fig. S2 for non-standardized SHG measurements). Unsurprisingly, we observed that SHG scoring displayed a dissimilar distribution of SHG values between surgical and needle biopsies in the F0-Metavir stage because of small variations in the fixation/waxing protocol. In order to ensure quantification homogeneity between surgical and needle biopsies, the average values of the SHG score corresponding to the F0-Metavir samples were, respectively, subtracted in both types of biopsy. This process allowed measurement standardization (normalized SHG scoring) by removing non-specific SHG signals mainly due to sample preparation (Fig. 5D).

By considering normalized SHG scoring, a Fibrosis-SHG index was defined (Fig. 6 and Table 1). The scoring method enabled the establishment of a gradation reflecting the four Fibrosis-Metavir stages but with the advantage of displaying a continuous scale leading to a more resolved evaluation of liver fibrosis severity. Notably, no effects of necroinflammation (A-Metavir) on SHG scoring were observed as presented in Supplementary Fig. 3. We analyzed the correlation between the Fibrosis-SHG index and the Fibrosis-Metavir score currently considered to be the gold standard in the assessment of liver fibrosis. As shown in

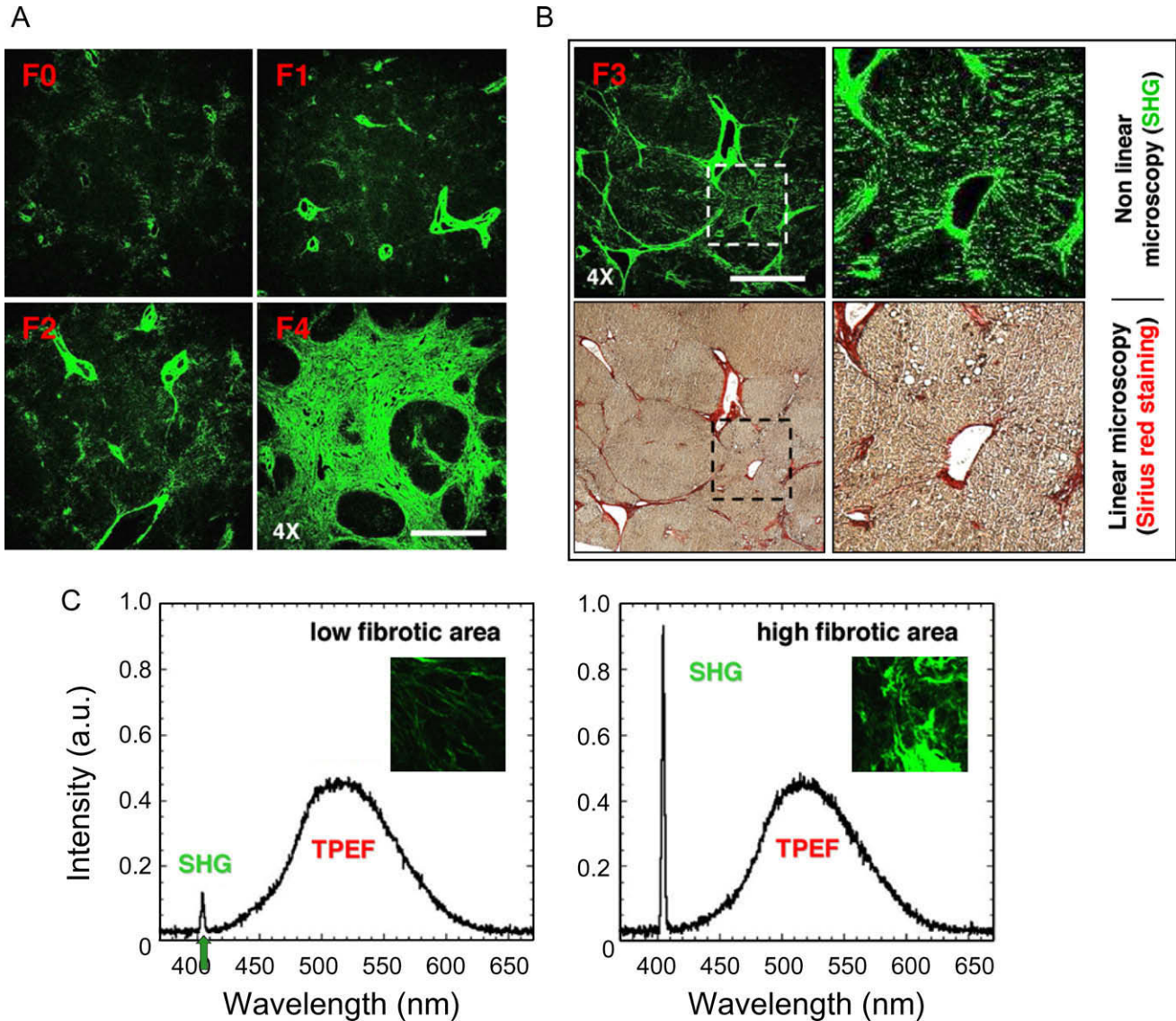


Fig. 4. SHG imaging in liver fibrosis progression. (A) SHG images representing the characteristic evolution of fibrillar collagen deposits from normal (F0-Metavir) to cirrhotic liver (F4-Metavir grade). F-Metavir grades have been determined by a pathologist using the Metavir scoring system. (B) Comparison between SHG imaging and linear microscopy after Sirius red staining (F3-Metavir biopsy). Right pictures show high magnification imaging performed in the area delimited by the dotted square. Samples were 5 μ m thick. Laser excitation: 100 mW with 810 nm wavelength; enlargement 4 \times ; scale bar: 1 mm. (C) TPEF and SHG spectra, respectively, recorded in non- and high fibrotic regions by using a 10 \times objective and a 10-fold zoom of the image. The corresponding SHG records are reported in the inserts.

Fig. 6, a significant correlation was found between the Fibrosis-Metavir stage and the Fibrosis-SHG index with a Spearman's coefficient of rank correlation for $\rho = 0.75$ ($p < 0.0001$). Interestingly, the Fibrosis-SHG index did not present a linear progression but an exponential increase of medians and averages between each stage (F0 to F4-Metavir), with statistical differences ($p < 0.05$) except between F1 and F2 stage where the p -value was just above statistical significance ($p = 0.0563$). In the earliest stages, SHG scores exhibited a progressive accumulation of fibrillar deposits (F0 to F2-Metavir) whereas fibrosis was characterized by a dramatic increase of fibrillar collagen in the last stages of the disease (F3-Metavir and cirrhosis F4 stages). The Metavir score is not linear, so the comparison to the SHG was thus not expected to be linear. As shown in Fig. 7, the technique

allowed for the distinction of patients with advanced fibrosis (moderate to severe) and cirrhosis. For discriminating between advanced (F2 to F4-Metavir) versus non-advanced fibrosis (F0 to F1-Metavir), the area under the curve was 0.88 (95% confidence interval: 0.81–0.93, $p < 0.0001$) (Fig. 7A). According to receiver operating characteristic (ROC) curve analysis, the best compromise between sensitivity (85.3%, 95% confidence interval: 75–93) and specificity (82.4%, 95% confidence interval: 69–92) was found for a threshold of 3.358 (Fibrosis-SHG index). For discriminating between cirrhosis (F4-Metavir) versus non-cirrhotic stages (F0 to F3-Metavir), the area under the curve was 0.89 (95% confidence interval: 0.81–0.94, $p < 0.0001$) (Fig. 7B). According to the ROC curve analysis, the best compromise between sensitivity (89.3%, 95% confidence interval: 72–98) and specificity

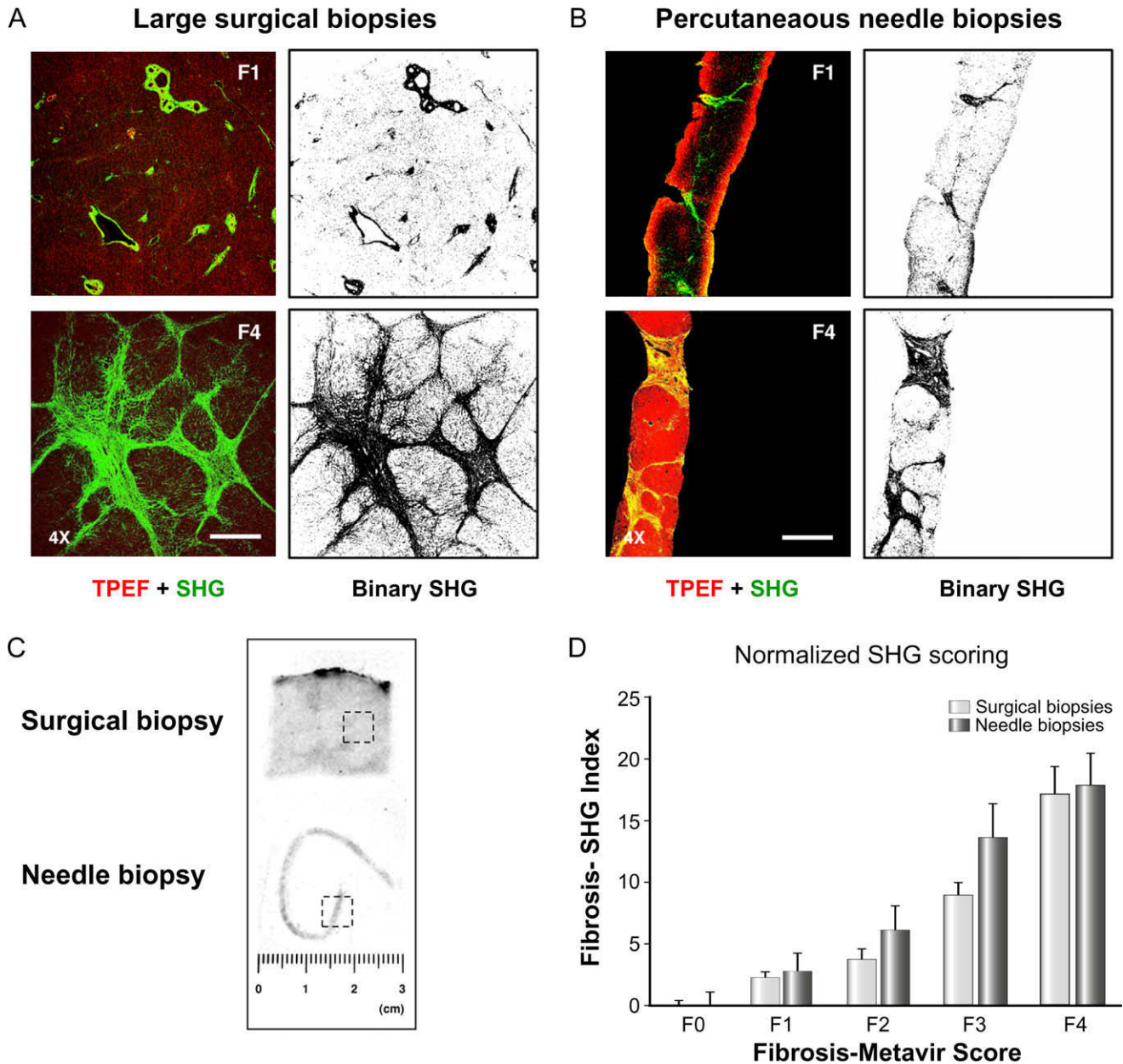


Fig. 5. Fibrillar collagen quantification by second harmonic microscopy: SHG scoring in human liver. Simultaneous TPEF/SHG acquisitions have been performed using circular polarization and SHG signals selectively processed to obtain a binary distribution of SHG after thresholding (fibrotic pixels in black). Input laser: 100 mW at 810 nm; 4× objective; scale bar: 1 mm. The scoring method is illustrated with F1 and F4-Metavir samples from surgical (A) and needle biopsies (B). (C) Surgical and needle biopsies. Dotted squares show the image field of the 4× magnification. (D) Standardized Fibrosis-SHG indexes determined for each F-Metavir stage, respectively, in 46 surgical biopsies ($n_{(F0)} = 9$, $n_{(F1)} = 10$, $n_{(F2)} = 7$, $n_{(F3)} = 10$, $n_{(F4)} = 10$) and 73 needle biopsies ($n_{(F0)} = 11$, $n_{(F1)} = 21$, $n_{(F2)} = 12$, $n_{(F3)} = 11$, $n_{(F4)} = 18$). Histograms indicate the average indexes \pm SEM after normalization. See Fig. S2 for distributions of non-normalized SHG ratios.

(77%, 95% confidence interval: 67–85) was found for a value superior to 7.247 in cirrhosis. Finally, the method offers the advantage of making the distinction of a number of fibrosis severities in the F4-Metavir grade. Indeed, F4-Metavir does not signify that it is twice the quantity of F2-Metavir in terms of the amount of fibrosis but is characterized by large variations of fibrotic deposits. In the cirrhosis stage, the degree of fibrosis can vary from 7.247 to more than 20 in term of SHG index. Using this new dynamic scale, fine distinctions in the measurement of cirrhosis can be made.

Discussion

Second harmonic microscopy presented a major challenge in the assessment of liver fibrosis. Our results demonstrate that SHG provides an original and powerful tool for the quantitative evaluation of fibrillar collagen deposits. We first validated the selectivity of SHG signals for fibrotic deposits (fibrillar collagen type I and III) in human liver by establishing a strong correlation between SHG and immunochemistry assays. According to the literature, immunolabelings of non-fibrillar collagen (type IV) and SHG signals did

Research Article

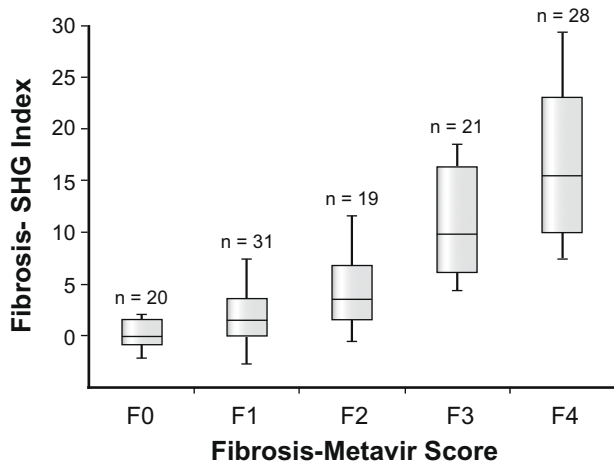


Fig. 6. Fibrosis-SHG index for histological assessment of fibrosis. The boxes indicate the median, 25th and 75th percentiles, whereas vertical bars display range of values. Fifty percent of values are comprised within the box, and eighty percent are comprised between the extremities of vertical bars. Mann-Whitney test indicates statistical differences between F0 and F1-Metavir stages ($p = 0.0322$), F2 and F3 ($p = 0.0036$), as well as F3 and F4 ($p = 0.0224$). SHG scoring shows an increase of medians and averages between F1 and F2-Metavir stages with p -value = 0.0563. The Spearman's coefficient of rank correlation for rho is 0.75 (95% confidence interval: 0.66–0.82, $p < 0.0001$).

not correlate as a result of the centrosymmetric organization of this component [11,19]. By using SHG scoring, we precisely quantified fibrillar collagen and fibrosis progression from the early to the advanced stages of the disease. Taking into consideration the two components of the Metavir scoring system, we found evidence for a strong correlation of Fibrosis-SHG index with F-Metavir whereas necroinflammation (A-Metavir) had no influence.

The SHG scoring method presents multiple advantages in comparison to the histologic numerical systems. The technique does not deteriorate or photo-damage samples, which enables its classic use in pathology after SHG scoring. Both SHG and TPEF imaging can be performed regardless of the manner of sample preparation. Both frozen fixed or paraffin embedded tissues (data not shown) can be used. In addition, the method is fast and easy to perform. Indeed, multiphoton microscopy does not require de-waxing or specific staining steps. After the calibration of the system, technical expertise is not required for SHG scoring and the methodology could be carried out in routine histopathology practices. Importantly, multiphoton imaging displays a high SHG signal-to-background ratio making specific detection of fibrillar collagen possible. SHG microscopy also allows for strong spatial resolution at the cellular level and 3-D reconstruction of the fibrillar collagen network with samples several hundred microns thick. High z-sectioning of SHG microscopy also makes the quantification of fibrillar collagen in a

well defined and standardized hyper-volume (x - y - z parameters) possible, regardless of irregularities in sample thickness. Moreover, 3-D imaging and orientation mapping of fibrillar collagen fibers would be a useful technology for the evaluation of ECM remodeling occurring in hepatic fibrosis. Finally, we cannot ignore the fact that sampling bias represents the limit of liver biopsy. Crucially, whereas classical histology provides fibrotic deposit information in a thin section (2-D), second harmonic microscopy allows for the capture of fibrillar collagen density in 3-D with a high in-depth resolution. Without altering samples, SHG scoring can be performed for an entire biopsy (data not shown). This property could contribute in greatly minimizing the sampling variations inherent to liver biopsies.

The major interest of SHG scoring is the standardization of measurement. The method is highly quantitative and provides a unique score (Fibrosis-SHG index) precisely reflecting the fibrosis level independently of operators, experimental conditions, or the biopsies' origin. A recent study showed significant disparities in the scoring of fibrosis between observers using the Metavir system, which increased between junior and qualified-senior academic pathologists [25]. The level of experience (specialization, duration, and location of practice) seemed to have more influence on the variability of Metavir scores than the characteristics of the biopsy itself. We tested reproducibility of the SHG measure by assessing similar biopsies at 3-day intervals using our standardized protocol (Fig. S4). Correlation between the first and second assessment was high with a rho = 0.988 ($p < 0.01$). SHG scoring also offers the possibility of discriminating between several levels of fibrosis within the same F-Metavir stage taking advantage of its continuous and dynamic gradation. Indeed, F4 samples displayed a large distribution of SHG scores and the determination of a sub-gradation inside the cirrhotic grade may allow for a distinction between low or high fibrotic F4 stages. The Fibrosis-SHG index needs to be compared with a scoring system exhibiting a quantitative continuous scale. We are currently designing a study in order to compare multi-parametric data including quantitative measurements of fibrosis such as histomorphometry of collagen, transient elastography and serum fibrosis markers, as well as Fibrosis-Metavir stage and SHG index. In addition, several etiologies including HBV, HCV and alcoholic livers will be considered.

SHG scoring gives the opportunity to quantify fibrosis regression in response to an antifibrotic treatment for validating experimental protocols especially for cirrhotic patients. Importantly, this method may greatly contribute to evaluating experimental treatments in rodent models in which fibrosis scoring is difficult due to the absence of well defined scores like the Metavir. We performed SHG and TPEF acquisitions successfully in various models of rodents (data not shown). Although essential factors conditioning fibrosis reversibility are not well known, a few treatments are currently under study [26,27] and could be precisely evaluated using SHG scoring. In this topic, the reticulation level

Table 1. Normalized scoring of fibrillar collagen by SHG in 119 liver biopsies.

Fibrosis - Metavir score	Percentage of total	Fibrosis - SHG index				
		25th percentile	75th percentile	Median	Mean	SEM
0 (n = 20)	16.8	-1.043	1.556	-0.127	0.000	0.571
1 (n = 31)	26.0	-0.168	3.620	1.451	2.571	0.988
2 (n = 19)	15.9	1.527	6.827	3.406	5.181	1.291
3 (n = 21)	17.6	5.993	16.330	9.812	11.331	1.594
4 (n = 28)	23.5	9.929	23.060	15.499	17.543	1.838
Total (n = 119)	100.0	-1.043	23.060	4.912	7.624	0.858

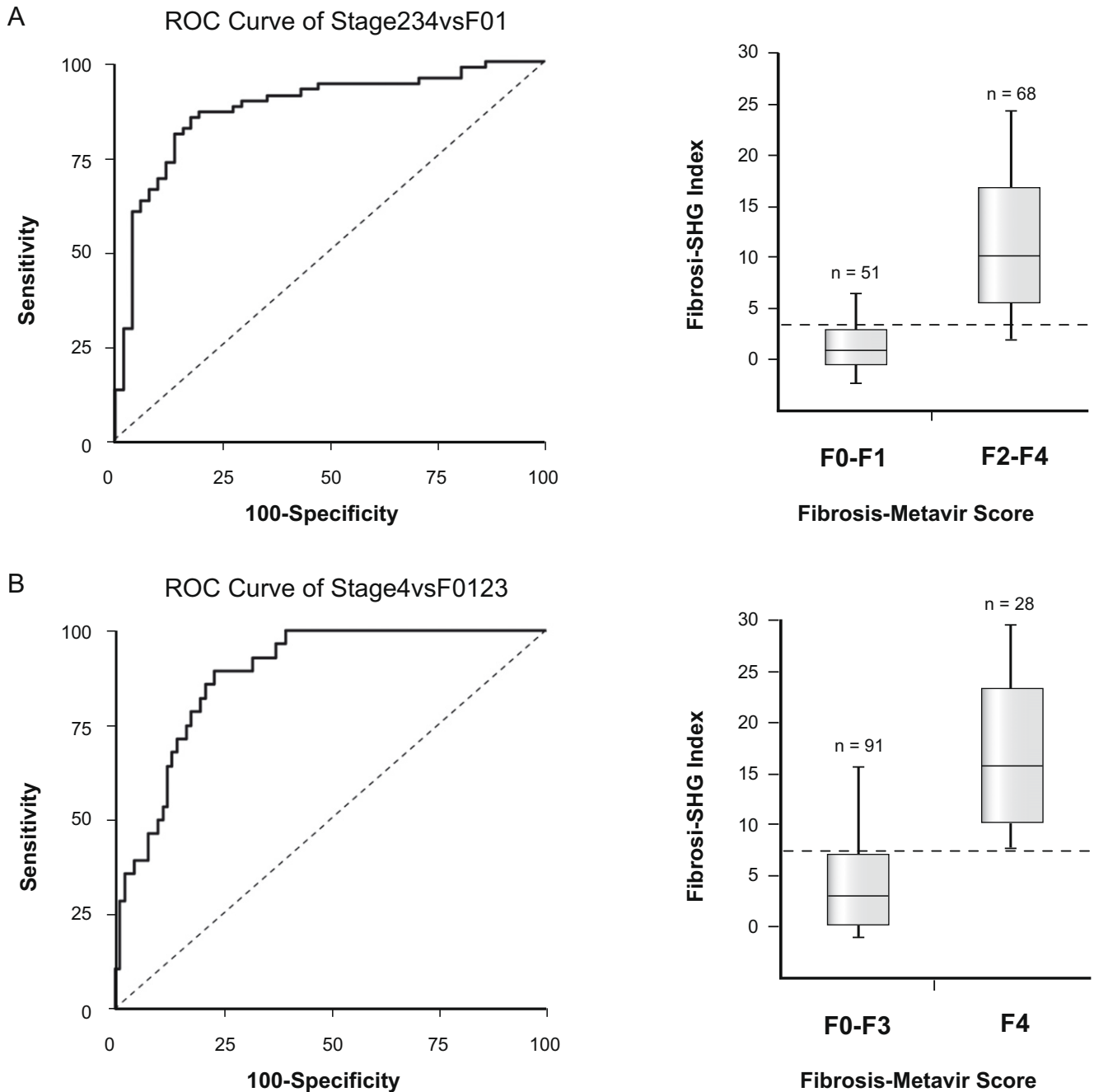


Fig. 7. ROC of Fibrosi-SHG index for the detection of (A) advanced fibrosis (moderate to severe) and (B) cirrhosis. (A) For discriminating between advanced (F2 to F4-Metavir) versus non-advanced fibrosis (F0 to F1-Metavir), the area under the curve was 0.88 (95% confidence interval: 0.81–0.93, $p < 0.0001$). (B) For discriminating between cirrhosis (F4-Metavir) versus non-cirrhotic stages, the area under the curve was 0.89 (95% confidence interval: 0.81–0.94, $p < 0.0001$). The dashed lines on box graphs represent the cut-offs for the detection of advanced fibrosis and cirrhosis.

of collagen also appears as a major event conditioning the possible regression of fibrosis. Indeed, a high reticulation may be associated with low reversibility and the determination of physical properties reflecting interactions between collagen fibers could greatly contribute to the identification of predictive factors conditioning liver fibrosis regression. We recently showed that polarimetric second harmonic microscopy allows the mapping of collagen fibril orientation in rodents and more generally in bio-

materials [28,29]. We are now developing this technology in order to assess the orientation fields of fibrillar collagen fibers in human liver to determine fibrils cross-links or collagen reticulation level with the intent of identifying patients predisposed to benefiting from an antifibrotic treatment (Fig. S5).

To conclude, this study demonstrates that second harmonic microscopy provides a valuable tool for an accurate assessment of human liver fibrosis. We anticipate that in the near future

Research Article

SHG imaging and fibrillar collagen scoring will be applicable to endoscopic systems by using optic fibers coupled with multiphoton microscopy, thus leading to a less invasive procedure for fibrosis evaluation. Undeniably, SHG technology offers a reliable method appreciably improving liver fibrosis assessment that could be easily applied in the diagnosis of several fibro-proliferative pathologies such as lung, kidney or cardiovascular diseases.

Acknowledgements

The authors thank the Histo-Pathology Platform (IFR 140), Pascale Bellaud for technical support in histologic preparation and staining, as well as Nina Cutro-Kelly for critical reading of the manuscript. We also thank Michel Samson, Claire Piquet-Pellorce and Mariette Lisbonne (EA SeRAIC), Anne Renault (UMR-CNRS 6251) and Pixel platform (UMR-CNRS 6026) for constructive comments on this study. We thank the CNRS project "Interface Physique, Chimie, Biologie: soutien à la prise de risque" for financial support.

Appendix A. Supplementary data

Supplementary data associated with this article can be found, in the online version, at [doi:10.1016/j.jhep.2009.12.009](https://doi.org/10.1016/j.jhep.2009.12.009).

References

- [1] Bataller R, Brenner DA. Liver fibrosis. *J Clin Invest* 2005;115:209–218.
- [2] Afdhal NH, Nunes D. Evaluation of liver fibrosis: a concise review. *Am J Gastroenterol* 2004;99:1160–1174.
- [3] Davis GL, Albright JE, Cook SF, Rosenberg DM. Projecting future complications of chronic hepatitis C in the United States. *Liver Transpl* 2003;9:331–338.
- [4] Scheuer PJ. Classification of chronic viral hepatitis: a need for reassessment. *J Hepatol* 1991;13:372–374.
- [5] Ishak K, Baptista A, Bianchi L, Callea F, De Groote J, Gudat F, et al. Histological grading and staging of chronic hepatitis. *J Hepatol* 1995;22:696–699.
- [6] The French METAVIR Cooperative Study Group. Intraobserver, interobserver variations in liver biopsy interpretation in patients with chronic hepatitis C. *Hepatology* 1994;20:15–20.
- [7] Poynard T, Mathurin P, Lai CL, Guyader D, Poupon R, Tainturier MH, et al. A comparison of fibrosis progression in chronic liver diseases. *J Hepatol* 2003;38:257–265.
- [8] Poynard T, Bedossa P, Opolon P. The OBSVIRC, METAVIR, CLINIVIR, and DOSVIRC groups. Natural history of liver fibrosis progression in patients with chronic hepatitis C. *Lancet* 1997;349:825–832.
- [9] Goodman ZD, Becker Jr RL, Pockros PJ, Afdhal NH. Progression of fibrosis in advanced chronic hepatitis C: evaluation by morphometric image analysis. *Hepatology* 2007;45:886–894.
- [10] Pilette C, Rousselet MC, Bedossa P, Chappard D, Oberti F, Rifflet H, et al. Histopathological evaluation of liver fibrosis: quantitative image analysis vs semi-quantitative scores. Comparison with serum markers. *J Hepatol* 1998;28:439–446.
- [11] Zipfel WR, Williams RM, Webb WW. Nonlinear magic: multiphoton microscopy in the biosciences. *Nat Biotechnol* 2003;21:1369–1377.
- [12] Gauderon R, Lukins PB, Sheppard CJ. Optimization of second-harmonic generation microscopy. *Micron* 2001;32:691–700.
- [13] Gauderon R, Lukins PB, Sheppard CJ. Simultaneous multichannel nonlinear imaging: combined two-photon excited fluorescence and second-harmonic generation microscopy. *Micron* 2001;32:685–689.
- [14] König K. Multiphoton microscopy in life sciences. *J Microsc* 2000;200:83–104.
- [15] Campagnola PJ, Loew LM. Second-harmonic imaging microscopy for visualizing biomolecular arrays in cells, tissues and organisms. *Nat Biotechnol* 2003;21:1356–1360.
- [16] Campagnola PJ, Millard AC, Terasaki M, Hoppe PE, Malone CJ, Mohler WA. Three-dimensional high-resolution second-harmonic generation imaging of endogenous structural proteins in biological tissues. *Biophys J* 2002;82:493–508.
- [17] Campagnola PJ, Clark HA, Mohler WA, Lewis A, Loew LM. Second-harmonic imaging microscopy of living cells. *J Biomed Opt* 2001;6:277–286.
- [18] Georgiou E, Theodossiou T, Hovhannisya V, Politopoulos K, Rapti GS, Yova D. Second and third optical harmonic generation in type I collagen, by nanosecond laser irradiation over a broad spectral region. *Opt Commun* 2000;176:253–260.
- [19] Boulesteix T, Pena AM, Pages N, Godeau G, Sauviat MP, Beaurepaire E, et al. Micrometer scale ex vivo multiphoton imaging of unstained arterial wall structure. *Cytometry A* 2006;69:20–26.
- [20] Brown E, McKee T, diTomaso E, Pluen A, Seed B, Boucher Y, et al. Dynamic imaging of collagen and its modulation in tumors in vivo using second-harmonic generation. *Nat Med* 2003;9:796–800.
- [21] Cox G, Kable E, Jones A, Fraser I, Manconi F, Gorrell MD. 3-Dimensional imaging of collagen using second harmonic generation. *J Struct Biol* 2003;141:53–62.
- [22] Zipfel WR, Williams RM, Christie R, Nikitin AY, Hyman BT, Webb WW. Live tissue intrinsic emission microscopy using multiphoton-excited native fluorescence and second harmonic generation. *Proc Natl Acad Sci USA* 2003;100:7075–7080.
- [23] Strupler M, Pena AM, Hernest M, Tharaux PL, Martin JL, Beaurepaire E, et al. Second harmonic imaging and scoring of collagen in fibrotic tissues. *Opt Express* 2007;15:4054–4065.
- [24] Pena AM, Fabre A, Debarre D, Marchal-Somme J, Crestani B, Martin JL, et al. Three-dimensional investigation and scoring of extracellular matrix remodeling during lung fibrosis using multiphoton microscopy. *Microsc Res Tech* 2007;70:162–170.
- [25] Rousselet MC, Michalak S, Dupre F, Croue A, Bedossa P, Saint-Andre JP, et al. Sources of variability in histological scoring of chronic viral hepatitis. *Hepatology* 2005;41:257–264.
- [26] Arthur MJ. Reversibility of liver fibrosis and cirrhosis following treatment for hepatitis C. *Gastroenterology* 2002;122:1525–1528.
- [27] Benyon RC, Iredale JP. Is liver fibrosis reversible? *Gut* 2000;46:443–446.
- [28] Odin C, Le Grand Y, Renault A, Gailhouste L, Baffet G. Orientation fields of nonlinear biological fibrils by second harmonic generation microscopy. *J Microsc* 2008;229:32–38.
- [29] Odin C, Guilbert T, Alkilani A, Boryskina OP, Fleury V, Le Grand Y. Collagen and myosin characterization by orientation field second harmonic microscopy. *Opt Express* 2008;16:16151–16165.